Quantitative Assessment of Apodized Square Aperture

A. T. Mohammed

Department of Astronomy, College of Science, University of Baghdad, Baghdad-Iraq.
Received:25/5/2005   Accepted: 17/4/2006

Abstract

Two-dimensional computer simulations are carried out to quantify the quality of apodized square aperture (ASA) in terms of the diffraction limited resolution and the efficiency of detection of faint companions. The study involve the quality of the point spread function (*psf*), and the modulation transfer function (MTF) of a reference star. Annular apodized square aperture (AASA) is also considered in this study. The results are then compared with the classical circular aperture.

ASA shows high contrast which increases the possibility of detection of faint companions and AASA demonstrates significant high frequency components which leads to high resolution.

الخلاصة

تمت محاكاة نوعية الصور الفلكية المأخوذة بواسطة التلسكوبات البصرية الأرضية بأستخدام فتحة

تلسكوب على شكل Apodized Square وكذلك على شكل Annular Apodized Square.

أن هذه الدراسة أخذت بنضر الأعتبار نوعية دالة الأنتشار النقطية ودالة التضمين الأنتقالية لمصدر نقطي.

Introduction

All telescopes have an inherent limitation to their angular resolution due to the diffraction of light at the telescope aperture. The diffraction of electromagnetic waves causes an optical system to behave as a low-pass filter in the formation of an image. The cut-off frequency is directly determined by the shape and size of the limiting pupil in the optical system. Telescope aperture and consequently the value of the cut-off frequency or knowledge of the psf and equivalently the MTF, is a fundamental importance in optical imaging, and has long been recognised as an important element in image analysis. The MTF, a quantitative measure in image quality, is describing the ability of a system to transfer object contrast to the image. The MTF describes the image structure as a function of its spatial frequencies. In some cases, we need to maximize the resolution of optical system in the specific frequency range which we are interested.

There are several criteria for analysing the performance of an optical imaging systems. The Rayleigh criterion is generally regarded as a fundamental limit in predicting the performance of optical imaging systems. In addition to that criterion, measurements of MTF, strehl ratio, diffraction limited resolution are also very well considered in quantifying optical systems [1-9].

The search to direct image an extrasolar planet requires contrast levels of 10^9 a few λ/D from the central star [10]. Scattered light in a telescope and diffraction pattern of the telescope's aperture limit the contrast possible for direct detection of faint companions. The circular aperture of telescope creates a sub-optimal diffraction pattern, the so called Airy pattern which is a zimuthally symmetric.

Apodized square aperture is firstly proposed by Nisenson & Papaliolios [11] in order to allow efficient detection of terrestrial extrasolar planets [12].

The aim of this paper is to assess the quality of ASA and the proposed AASA in terms of the contrast and resolution.

Theory

In this section, we present a brief and simple theory of the image formation model. The fundamental equation to be used for the formation of an image by an ideal optical system is given by:

$$i(x,y) = \int\int_{-\infty}^{\infty} o(x',y')\, psf(x-x',y-y')\, dx'dy' \quad (1)$$

$$i(x,y) = o(x,y) \otimes psf(x,y) \quad (2)$$

Equation (1) and (2) are equivalent. They are representing a convolution equation. Where $i(x,y)$ is the observed image intensity, $o(x,y)$ is the object intensity, $psf(x,y)$ represents the image blurring function caused by an optical system and $\otimes$ denotes convolution operator. The Fourier transform of eq.(2) is given by:

$$I(u,v) = O(u,v).\, T(u,v) \quad (3)$$

where $I(u,v)$ and $O(u,v)$ are, complex Fourier transforms of the image intensity $i(x,y)$, and the object intensity $o(x,y)$ respectively; $T(u,v)$ which represents the Fourier transform of the *psf*, is an important function known as the optical transfer function (*OTF*). The modulation or amplitude of the complex function $T(u,v)$ is called MTF. In general, the resolution of an imaging system is limited only by the luck of large optical elements that are free from inherent distortions.

Now consider an extremely distant quasimonochromatic point source located on the optical axis of a simple imaging system. In the absence of atmospheric turbulence, this source would generates a plane wave normally incident on the lens. In the presence of the atmosphere, the plane wave incident on the inhomogeneous medium propagates into the medium, and ultimately a perturbed wave falls on the lens. The field distribution incident on the lens can be expressed as,

$$U(\eta,\gamma) = e^{i\phi(\eta,\gamma)} \quad (4)$$

where $\phi(\eta,\gamma)$ is the random phase of the incident wavefront and the variables (η,γ) represent distances in the pupil function. The instantaneous *psf* of the entire telescope atmosphere system is given by:

$$psf(x,y) = \left| FT\, [\, H(\eta,\gamma)\, U(\eta,\gamma)\,] \right|^2 \quad (5)$$

where $H(\eta,\gamma)$ represents the pupil function and *FT* denotes *Fourier Transform* operator. The corresponding *OTF* is the *Fourier Transform* of the *psf*, thus

$$T(u,v)=FT[psf(x,y)] \quad (6)$$

Equation (6) can also be written in terms of the pupil function and the field distribution incident on the lens as,

$$T(u,v) = \int\int_{-\infty}^{\infty} H(\eta,\gamma)H^*(\eta-\eta',\gamma-\gamma')$$
$$.U(\eta,\gamma)U^*(\eta-\eta',\gamma-\gamma')d\eta'd\gamma' \quad (7)$$

where * denotes complex conjugate. The variables η and γ are related to the Fourier space variables u and v by $\eta = \lambda f u$, $\gamma = \lambda f \upsilon$, where λ is the wavelength and f is the focal length [10,11].

Results and Discussions

The pupil function $H(\eta,\gamma)$ is taken to be a two-dimensional circular function via the following equation:

$$H(\eta,\gamma) = \begin{cases} 1 & \text{if} \quad R_1 < [(\eta-\eta_c)^2 + (\gamma-\gamma_c)^2]^{\frac{1}{2}} \leq R \\ 0 & \text{elsewhere} \end{cases} \quad (8)$$

Where R_1 & R are the radii of the inner and outer circles. η, γ are 2-D coordinates in the pupil plane, and η_c, γ_c represent the center of an array.

$$\in = \frac{R_1}{R}$$

The actual size of the array (M by N) is taken to be 512 pixels by 512 pixels. This size is taken as large as possible in order to keep the theoretical diffraction limit of these apertures to be truncated at zero values inside this array. In addition to that, this size of array will reduce the error that associated with the simulation of the aperture. This error is due to the artifact that arise from the rough edges of the aperture. Eq.(8) was used to generate circular aperture at different values of $\in$ as shown in Fig.(1). It should be pointed out here that R is taken to be 128 pixels to generate the results throughout this paper.
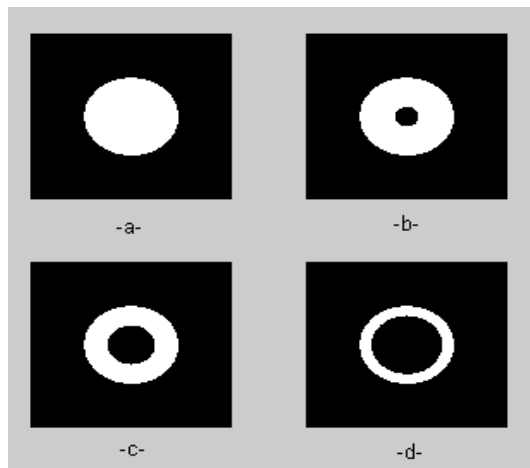
Fig.1: Circular aperture at different values of $\in$
  a- $\in$ **=0, b-** $\in$ **=0.25, c-** $\in$ **=0.5, d-** $\in$ **=0.75**

The apodized square aperture (ASA) is given by:

$$H(\eta, \gamma) = [1 - (\frac{\eta - \eta_c}{R})^2]^v [1 - (\frac{\gamma - \gamma_c}{R})^2]^v \quad (9)$$

Where v is taken to be 1,2,3, and 4 respectively. The pupil transmission is zero everywhere except inside R where the above equation is taken place. Fig (2-I & II) show the ASA at different values of v and their normalised horizontal lines through the centers of their corresponding arrays.
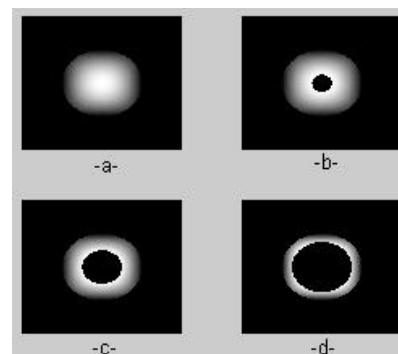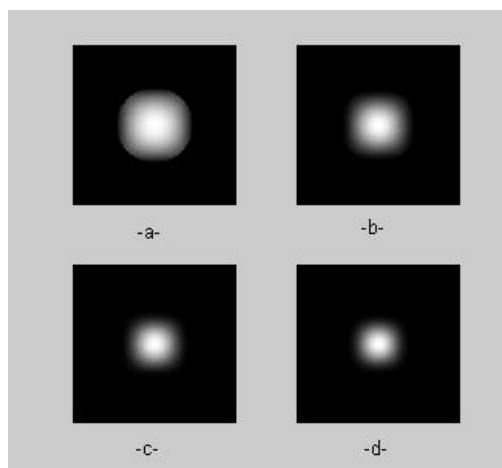
Fig.2-I: ASA at different values of v
    a- v=1, b- v=2, c- v=3 d- v=4

Fig.2-II: Central lines through Fig.2-I

**Fig.3: AASA (v=1) at different values
of** $\in$ **(0,0.25,0.5,0.75).**

Now, if we consider the object to be imaged is an extremely distant quasimonochromatic point source located at the axis of an optical telescope. In the absence of atmospheric turbulence, this source would generates a plane wave as mentioned before and so that $\phi(\eta, \gamma)$ in eq. (4) becomes zero and consequently $U(\eta, \gamma) = 1$.

The *psf*s of the above apertures are computed following eq.(5). The perspective plots of the central parts of the psfs are shown in Figs.(4 to 7). Figs.(8 to 11) show the central lines through Figs(4 to 7) respectively.
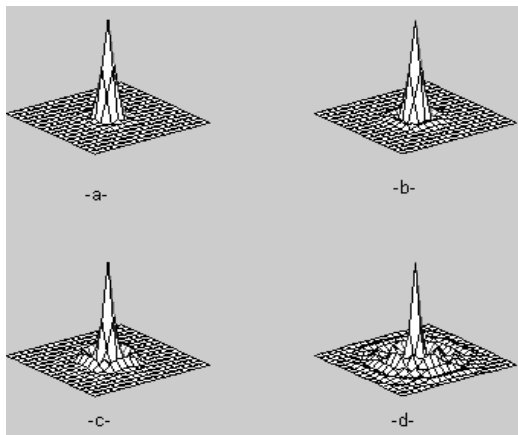
Fig.4: Perspective plots of the *psf* of circular aperture at different values of ∈ (0,0.25,0.5,0.75).

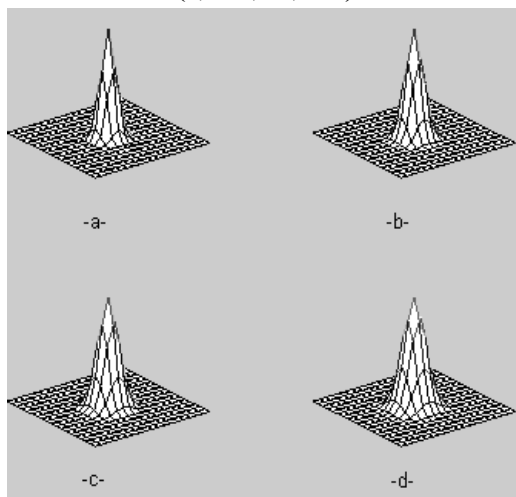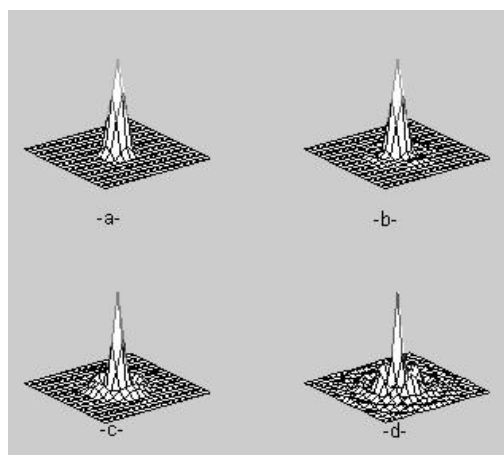**Fig.7: Perspective plots of the *psf* of AASA (v=4) at different values of ∈ (0,0.25,0.5,0.75).**

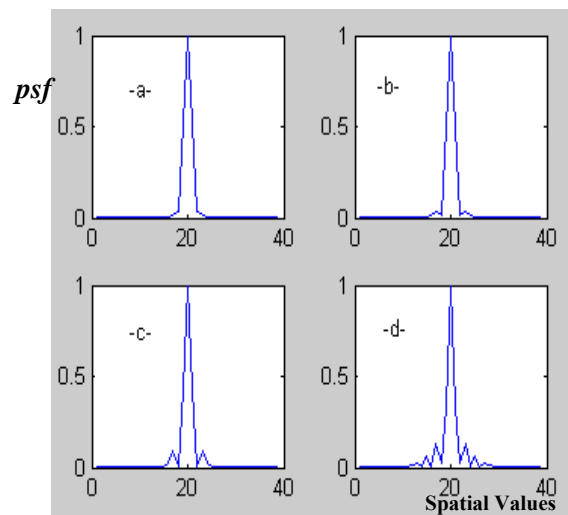**Fig.5: Perspective plots of the *psf* of ASA at different values of v (1,2,3,4).**

Fig.8: Horizontal lines through the central part of the actual *psf* of the circular aperture at different values of ∈ (0,0.25,0.5,0.75).
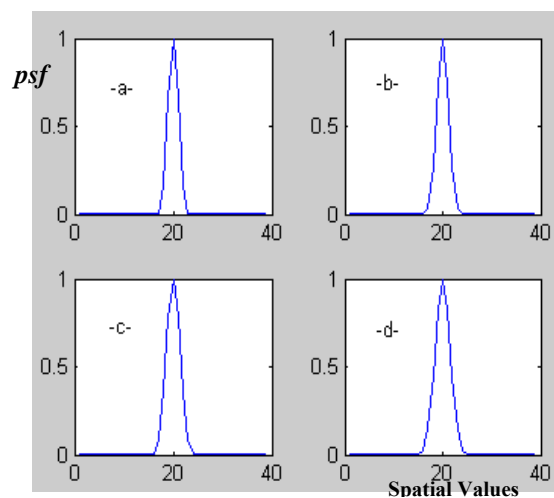

Fig.6: Perspective plots of the *psf* of AASA (V=1) at different values of ∈ (0,0.25,0.5,0.75).

Fig.9: Horizontal lines through the central parts of the actual *psfs* of the ASA at different values of v (1,2,3,4).
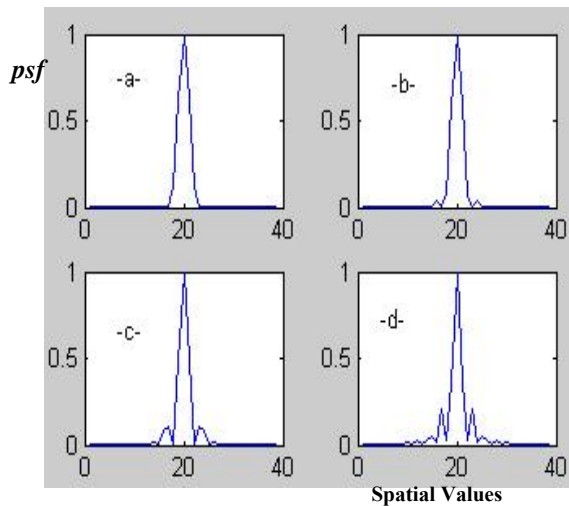
Fig.10: Horizontal lines through the central parts of the actual *psfs* of the AASA (*v*=1) at different values of ∈ (0,0.25,0.5,0.75).
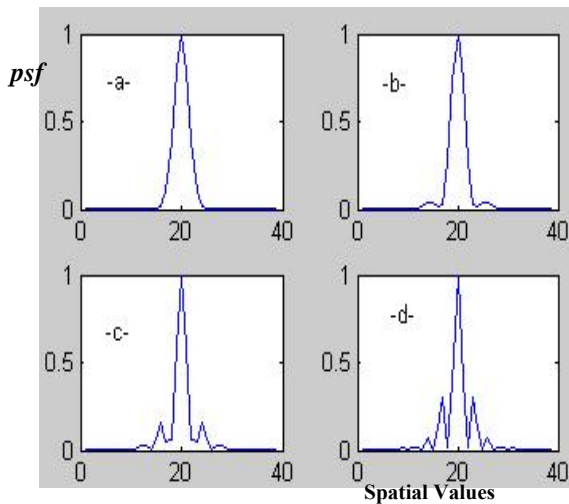

Fig.11: Horizontal lines through the central parts of the actual *psfs* of the AASA (*v*=4) at different values of ∈ (0,0.25,0.5,0.75).

The figures from 4 to 9 demonstrate significantly the advantage of using ASA and AASA. The central spike is very narrow as shown in Figs.(10-d & 11-d) compared with all other central spikes but the secondary spikes are larger that others. In case of defining resolution, the radius of the diffraction spike (central spike) is considered.

The contrast of the regions of the psf is defined by:

$$Z = psf(x,y) / psf(0,0) \qquad (10)$$

Where $psf(0,0)$ is the intensity of the center of the array of the *psf* (peak intensity).

The contrast along the horizantal line passing the image center at different values of v and ∈ are shown in Figs.(12 to 15). It should be pointed out here that the contrast is taken in logarithmic scaling.
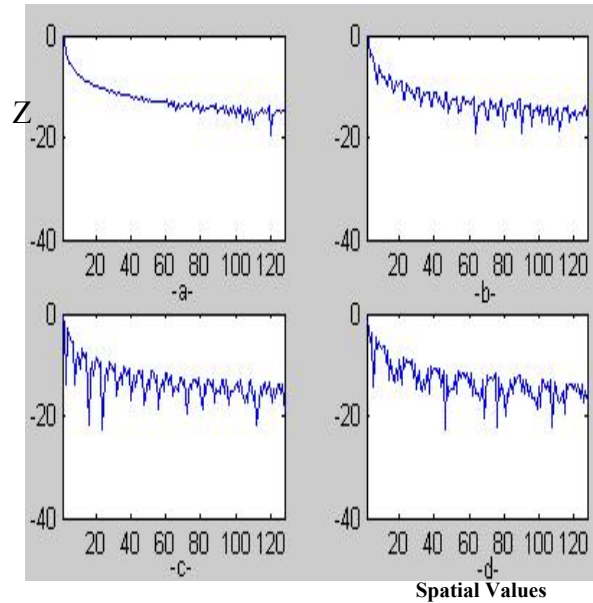

Fig.12: Horizontal cuts along the intensity of the *psfs* of the circular aperture at different values of ∈(0,0.25,0.5,0.75).
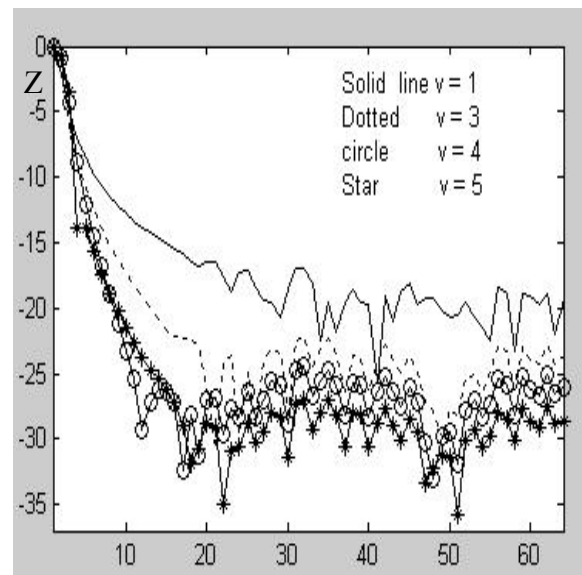

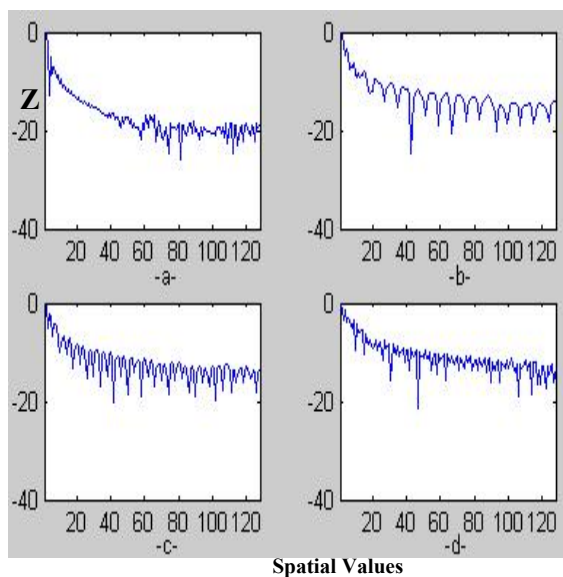**Fig.13: Horizontal cuts along the intensity of the *psfs* of ASA at different values of *v***

Fig.14: Horizontal cuts along the intensity of the *psfs* of ASA (*v*=1) at different values of ∈ (0,0.25,0.5,0.75).
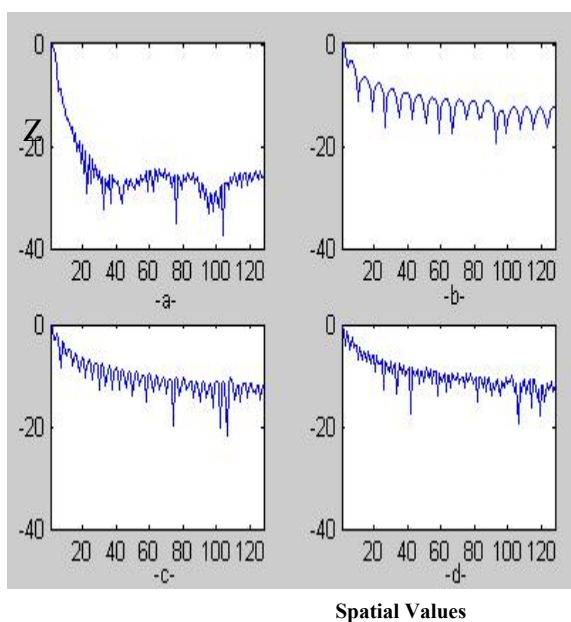

Spatial Values
Fig.15: Horizontal cuts along the intensity of the *psfs* of ASA (*v*=4) at different values of ∈ (0,0.25,0.5,0.75).

The above figures show very clearly the locations where high contrast occurs (i.e., image area is much darker than other area) . ASA demonstrates the superiority of producing high contrast image with *v* > 3.

The MTF is computed via eq.(6) or eq.(7) which represents the autocorrelation of the pupil function. The corresponding MTFs are shown in Figs.(16 to 19).
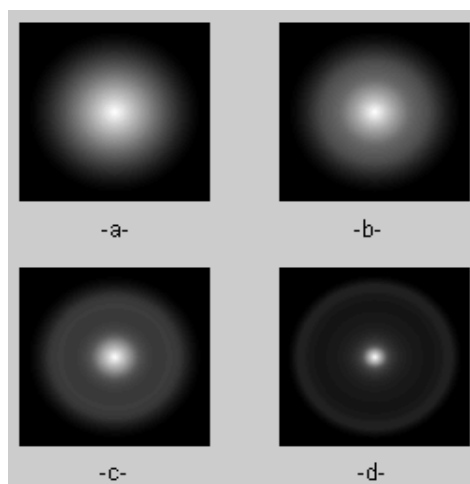

Fig.16: MTFs of the circular aperture at different values of ∈ (0,0.25,0.5,0.75). .
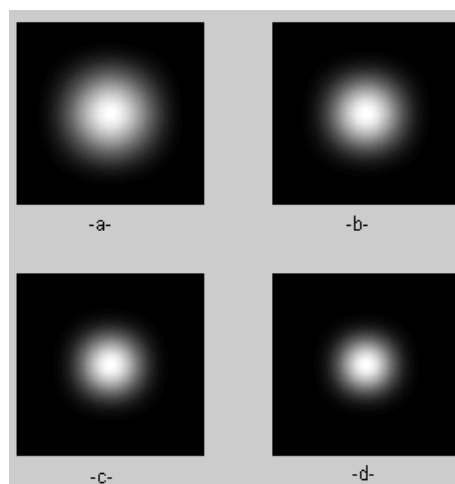

Fig.17: MTFs of ASA at different values of *v* (1,2,3,4).
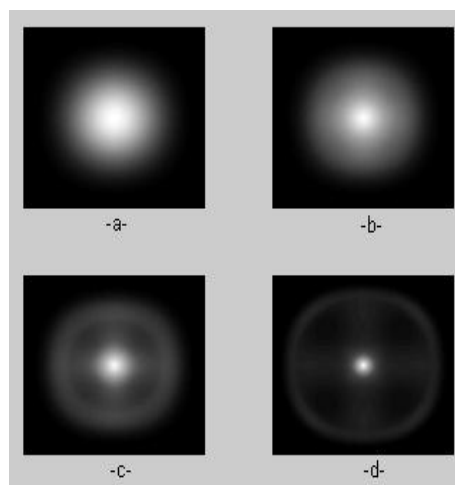

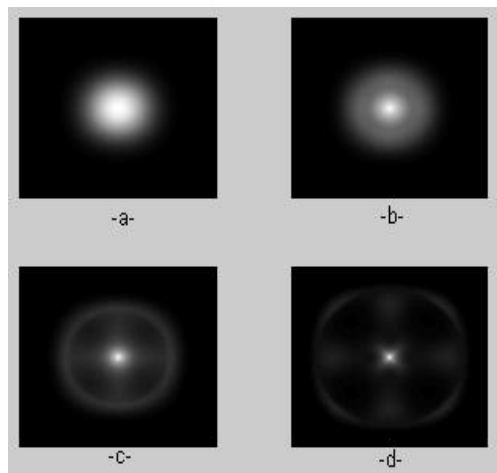**Fig.18: MTFs of AASA (*v*=1) at different values of ∈ (0,0.25,0.5,0.75).**

Fig.19: MTFs of AASA (*v*=4) at different values of ∈ (0,0.25,0.5,0.75).

Fig.22: Horizontal lines through the central images of Fig.18

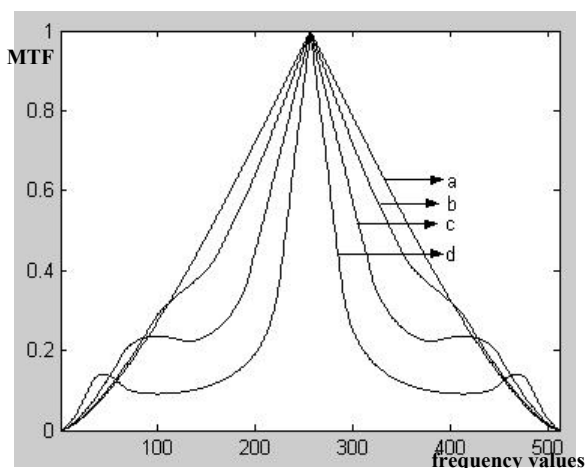The normalised central plots of MTF of Figs.(16 to 19) are shown in Figs.(20 to 23) respectively.

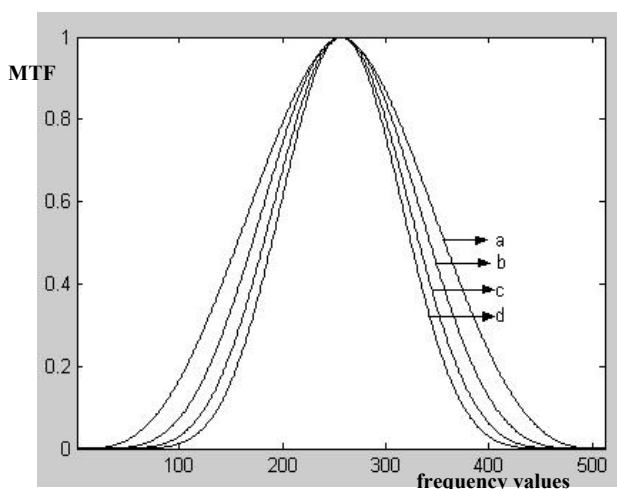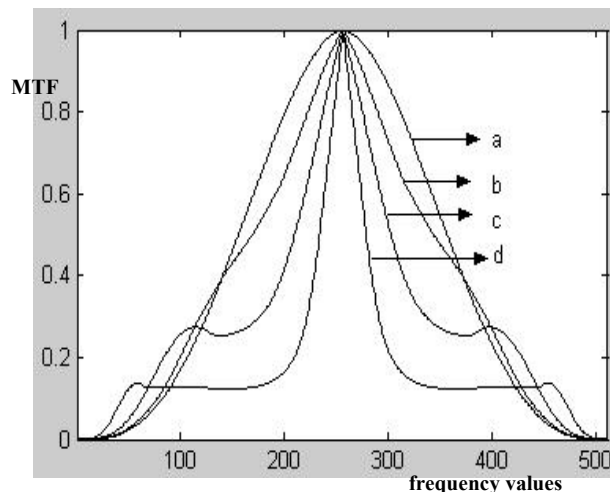**Fig.20: Horizontal lines through the central images of Fig.16**
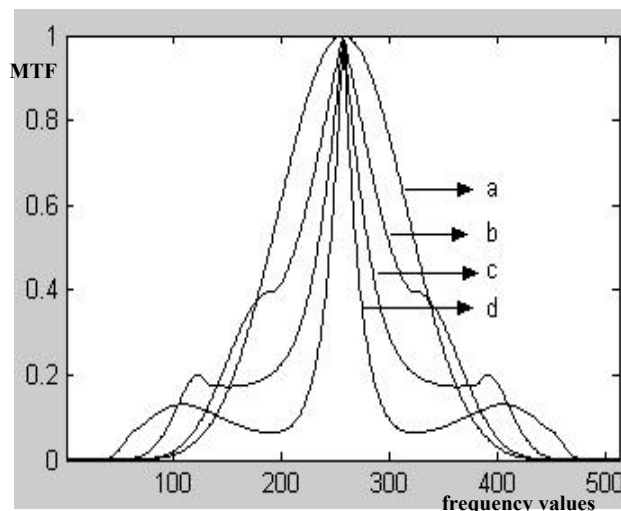

Fig.23: Horizontal lines through the central images of Fig.19

Fig.(19) illustrates significantly the high frequency components that produced by AASA (*v*=1 & 4) at ∈=0.75

The average frequency components of the normalised MTF (AF) for each aperture is calculated via the equation,

$$AF = \frac{1}{MN} \sum_{y=1}^{M} \sum_{x=1}^{N} MTF(x, y) \qquad (11)$$

Table (1): AF for the described apertures.

∈	Circular aperture	AASA (*v*=1)	AASA (*v*=4)	*v*	ASA
0	0.1962	0.1605	0.0759	1	0.1605
0.25	0.1840	0.1514	0.0723	2	0.1203
0.5	0.1472	0.1235	0.0612	3	0.0935
0.75	0.0859	0.0744	0.0401	4	0.0759

Fig.21: Horizontal lines through the central images of Fig.17

201

The table and fig.23 describe the essential amount of high frequency components that produced with AASA.

Conclusions

The following conclusions could be drawn:

1-As *v* increases, the actual width of the *psf* increases.

2-The central spike of AASA (*v*=4) at ∈=0.75 is sharper than any other central spikes.

3-The contrast of AASA becomes higher as *v* increases. In this case, some of the image area is much darker than the other areas. This will allow deep search for faint companions. For *v* > 3, the increases in contrast becomes insignificant.

4-AASA (*v*=1 & 4) show the build up of the high frequency components as ∈ increases. This may be useful in stellar speckle interferometery.

5-Circular aperture with ∈=0 gives highest AF while AASA (*v*=4) with ∈=0.75 gives lowest *AF*.

References

1. C. William and O. Becklund, *"Introduction to the optical transfer function"*, Wiley Series in Pure and Applied Optics, **1989**.
2. J. E. Harvey and C. Ftaclas, *"Diffraction effects of telescope secondary mirror spiders on various image quality criteria"*, Applied Optics, Vol.34, No. 28, pp. 6337-6349, **1995**.
3. T. A. Brummelaar and W. G. Bagnuolo, *"Strehl ratio and visibility in long baseline stellar interferometry"*, Optics Letters, Vol. 20, pp. 521-523, **1995**.
4. T. A. Brummelaar, W. G. Bagnuolo, and S. T. Ridgway, *"Strehl ratio and Coherence loss in long baseline interferometry"*, Chara Technical Report, Center for High Angular Resolution Astronomy, Georgia State University, No. 6, 15 Dec. **1994**.
5. J. E. Baldwin, R. N. Tubbs, G. C. Cox, C. D. Mackay, R. W. Wilson, and M. I. Anderson, *"Diffraction limited 800 nm imaging with 2.56 m Nordic Optical Telescope"*, Astronomy & Astrophysics 368, L1-L4, **2001**.
6. Sergio Granieri, E. Enrique, and W. D. Furlan, *"Performance analysis of optical imaging systems based on the fractional Fourier transform"*, Journal of Modern Optics, Vo. 45, No. 9, pp. 1797-1807, **1998**.
7. Jean-Marc Delvit, Dominique Leger, Sylvie Rogues, and Christophe Valorge, *"Modulation transfer function estimation from non specific images"*, Optical Engineering 43(06), pp. 1355-1365, Donal F. O'shea; Ed., June **2004**.
8. Jong Sup Song, Yun Woo Lee, Jae Bong Song, In Won Lee, Ho-Soon Yang, Young-Wan Choi, and Jae Heungo Jo, *"Dual testing of a large aperture optical system"*, Proc. SPIE, Interferometry XI:Applications, Vol. 4778, pp. 227-236; Wolfgang Osten; Ed., June **2002**.
9. David Carpenter, Soonjo Chung, *"Adaptive optical system"*, Massachusetts Institute of Technology, MIT Space System Laboratory, 4 December **2000**.
10. John Debes, astro-ph 0301051 v1, 3 Jan **2003**.
11. Nisenson P. & Papaliolios C. APJ , 548, L201, **2001**.
12. Olivier Guyon, Astronomy & Astrophysics, April **2003**.